Anal. Chem. **1998,** *70,* 3735−3741

Hadamard Transform Time-of-Flight Mass Spectrometry

Ansgar Brock, Nestor Rodriguez, and Richard N. Zare*

Department of Chemistry, Stanford University, Stanford, California 94305

A new mode of operation of a time-of-flight mass spectrometer (TOFMS) is described and demonstrated. A continuous ion beam emerging from the ion source is accelerated and then modulated by a pseudorandom sequence of "on" and "off" pulses. The data acquisition period is set to match the period of the modulation sequence, and data are acquired synchronously with the modulation of the ion beam. The modulation sequence is deconvoluted from the data using a fast Hadamard transform (FHT) algorithm to extract the time-of-flight distribution of the ions. This multiplexing scheme increases the ion usage to ∼50% for a single detector instrument and ∼100% for a multiple detector instrument, which improves the signal level considerably over that of conventional TOFMS. The gains in signal lead to an improved signal-to-noise ratio or alternatively reduced data acquisition time, giving HT-TOFMS a major instrumental advantage over conventional TOFMS in a number of applications at little additional cost. Positive mode electrospray ionization mass spectra of tetrabutylammonium perchlorate, cesium chloride, and a protein mixture of cytochrome *c* and ubiquitin are presented to illustrate the method and the device.

Today, a large number of mass spectrometric methods are in use. As applications vary, so do instruments. Fourier transform ion cyclotron mass spectrometry (FT-ICRMS) is the method of choice if ultimate sensitivity and resolution is required.[1,2] FT-ICRMS offers, in addition, the ability to carry out mass spectrometry/mass spectrometry (MS/MS) experiments. A sector instrument consists of a combination of magnetic and electric resolving stages. This is probably the oldest type of mass spectrometer. Sector instruments also give high resolution and are a standard MS tool. Quadrupole mass analyzers are widely distributed and are found in multistage instruments, which are often used for structure elucidation as well as low-resolution, single-stage, general-purpose detectors. The compactness and modest cost of a quadrupole mass analyzer are reasons for its proliferation in residual gas analyzers (RGAs) and benchtop gas chromatography/mass spectrometry equipment. Quadrupole ion trap instruments, another dynamic mass spectrometer, are becoming more popular as general-purpose mass spectrometers and detectors.[3,4] Their low-vacuum requirements, small size, and MS/MS capabilities are very desirable properties. Time-of-flight mass spectrometers (TOFMS) have seen a renaissance since the mid-1980s. This rebirth was accompanied by the emergence of new ionization techniques such as two-step laser desorption/laser ionization mass spectrometry (L^2MS)[5,6] and matrix-assisted laser desorption/ionization (MALDI).[1,7] Also, the interest in the study of always larger molecules and clusters demanded high-mass-range capabilities, which are not easily achieved with other instruments. Remarkably, TOFMS instrumentation could never capture its share in the growing market for chromatography/mass spectrometry instrumentation, even though TOFMS has the desirable properties of high ion transmission, essentially unlimited mass range, high repetition rate, good resolution, and modest cost.[8] TOFMS is certainly set apart from other MS methods that are hampered by a resolution/transmission compromise. In contrast, improved resolution in TOFMS should also lead to improved sensitivity, because ion transmission is unaffected.

The standard way to operate a TOFMS[8] is to produce an ion packet and then accelerate the ions in the packet to the same energy and let them drift in a field-free region of fixed length where they disperse in time. The detector signal is recorded as a function of time by some type of wave form recorder and represents directly the time-of-flight distribution of the ions, which is easily converted into a mass spectrum by means of a square root relationship that links flight time and mass for ions of the same energy. After the dispersed ion packet has arrived at the detector, the experiment is repeated. For optimum resolution, the initial ion packet should be spatially confined as much as possible into a plane normal to the accelerating fields and have a low kinetic energy spread. This mode of operation matches ideally TOFMS to ionization schemes in which ions are produced internally, that is, in the acceleration region of the mass analyzer, and ionization is confined to a very short time interval as in laser

(1) Castro, J. A.; Wilkins, C. L. *Anal. Chem.* **1993**, *65*, 2621−2627.
(2) Valaskovic, G. A.; Kelleher, N. L.; McLafferty, F. W. *Science* **1996**, *273*, 1199−1202.
(3) McLuckey, S. A.; Berkel, G. J. V.; Glish, G. L.; Huang, E. C.; Henion, J. D. *Anal. Chem.* **1991**, *63*, 375−383.
(4) March, R. E., Todd, J. F. J., Eds. *Practical aspects of ion trap mass spectrometry*; CRC Series Modern Mass Spectrometry; CRC: Boca Raton, FL, 1995.
(5) Clemett, S. J.; Zare, R. N. *Int. Astron. Union Symp. (Netherlands)* **1996**, *178*, 305−320.
(6) Kovalenko, L. J.; Philippoz, J.-M.; Bucenell, J. R.; Zenobi, R.; Zare, R. N. *Space Sci. Rev.* **1991**, *56*, 191−195.
(7) Cornish, T.; Cotter, R. J. *Rapid. Commun. Mass Spectrom.* **1992**, *6*, 242−248.
(8) Cotter, R. J., Ed. *Time-of-Flight Mass Spectrometry*; ACS Symposium Series 547; American Chemical Society: Washington, DC, 1994.

S0003-2700(98)00403-X CCC: $15.00
Published on Web 08/20/1998

ionization. If a continuous ion source is to be employed, this mode of operation results in low ion usage, because ions are not measured during the time an ion packet disperses in the field-free region of the instrument. In addition, for an external ion source, the problem of bringing the ions into the acceleration region with little spatial and energetic spread must be solved.

Different investigators have tackled the problem of interfacing a continuous external ion source to a TOFMS. The most obvious solution is the use of an ion trap[9] to store most of the ions that are produced during the time a packet disperses in the field-free region and then pulse the stored ions from the trap and accelerate them. This method seems appealing, but continuous trapping of an ion beam in an ion trap is itself not a straightforward procedure.[10,11] In addition, the ion trap has added essentially another mass spectrometer and the costs thereof to the instrument.

Another approach to achieve at least some ion storage is to produce a low-energy ion beam and let it drift orthogonally to the time-of-flight axis into a field-free region during the time an ion packet disperses in the analyzer.[12−14] This approach requires the handling of a low-energy ion beam, which can be problematic, and the possibility of a mass-dependent extraction duty cycle.[14] Although this approach seems to work well in a number of laboratories,[14−16] we believe we have found a superior approach involving multiplexing.

Our approach is to apply a pseudorandom sequence of pulses to a planar grid through which the ions pass. With the pulse "on" corresponding to no potential difference between the wire elements of the grid, the ions are transmitted in an undeflected manner to a detector. With the pulse "off" corresponding to a potential difference between the wire elements of the grid, the ions are deflected onto two locations to either side of the detector. Hence, for a single detector system located at the position of the undeflected ions, the duty cycle is 50% if losses from the grid are neglected; and for a multiple detector system that captures both the deflected and the undeflected ions, the duty cycle is 100%. The pulse sequence is deconvoluted numerically from the detector signal to yield the mass spectrum by means of a Hadamard transform. We call this procedure Hadamard transform time-of-flight mass spectrometry (HT-TOFMS). Pseudorandom pulse sequences have been used previously in neutron scattering,[17] molecular beam−surface scattering,[18] and reactive scattering[19] experiments of neutral species. In these experiments, modulation is achieved by interrupting the beam with a mechanical chopper possessing a pseudorandom tooth pattern.[18] There the method is better known under the synonyms "pseudorandom time of flight" or "cross-correlation time of flight". Another more general name that relates to this type of multiplexing is pseudonoise spectroscopy. We chose the name Hadamard transform time-of-flight mass spectrometry to relate it more to the realm of optical spectroscopy where the multiplexing scheme is known as Hadamard spectroscopy[20] and Hadamard transform optics.[21] In addition, the name evokes its cousin, Fourier transform spectroscopy, which is another, more familiar multiplexing method. Although the Hadamard transform technique has been proposed for ion mobility spectrometry (IMS),[22] it has never before been used successfully in time-of-flight mass spectrometry, which is an altogether different application than IMS.

Multiplexing schemes for TOFMS have been considered in the past.[23] Surprisingly, no connection was made to nuclear and optical spectroscopic methods that previously were used to solve similar problems. In 1971, Bailey et al.[24] attempted to improve the sensitivity of a RGA using a miniaturized time-of-flight mass spectrometer in which a random set of pulses were encoded in the transmitted ions (at an unstated repetition rate) and decoded at the detector using an analog cross-correlation technique. Pulses with varying delay times were applied to pairs of grids located along the flight axis at the entrance and just before the detector. Unfortunately, no significant sensitivity gain was achieved. The cause of the failure was excessive electronic noise according to the authors. In 1986, Knorr and co-workers[25] introduced Fourier transform time-of-flight mass spectrometry (FT-TOFMS) after having demonstrated multiplex gains the year before in Fourier transform ion mobility spectrometry (FT-IMS).[26] The instrumental setup, which is based on the ion mobility spectrometer, was rather complicated and failed to produce the theoretically predicted gains. The observed degraded performance of the FT-TOFMS as compared to the instrument operated in the pulsed mode can be explained by a number of experimental and theoretical considerations, some of which we discuss later. Most importantly, the changeover in the noise characteristics from being dominated by detector noise in FT-IMS to shot noise in FT-TOFMS was not mentioned by the authors. In 1995, Meyerholtz et al.[27] described a multiplexing procedure using a conventional time-of-flight instrument in which the Wiley−McLaren[28] extraction region involving a pair of grids is pulsed. In contrast to the work of Bailey et al.,[24] there is no pair of grids at the detector and the cross-correlation is carried out numerically. This scheme, however, is still seriously impaired in practive by the difficulty of implementing this procedure using a pair of grids and parameters allowing for space focusing. As can be recognized from Bailey et al.,[24] a

(9) Michael, S. M.; Chien, B. M.; Lubman, D. M. *Anal. Chem.* **1993**, *65*, 2614−2620.
(10) Koefel, P. In *Practical aspects of ion trap mass spectrometry*; March, R. E., Todd, J. F. J., Eds.; CRC: Boca Raton, FL, 1995; Vol. 2, pp 51−87.
(11) Moore, R. B.; Lunney, M. D. In *Practical aspects of ion trap mass spectrometry*; March, R. E., Todd, J. F. J., Eds.; CRC: Boca Raton, FL, 1995; Vol. 2, pp 263−302.
(12) Fang, L.; Zhang, R.; Williams, E. R.; Zare, R. N. *Anal. Chem.* **1994**, *66*, 3696−3701.
(13) Laiko, V. V.; Dodonov, A. F. *Rapid Commun. Mass Spectrom.* **1994**, *8*, 720−726.
(14) Boyle, J. G.; Whitehouse, C. M. *Anal. Chem.* **1992**, *64*, 2084−2089.
(15) Verentchikov, A. N.; Ens, W.; Standing, K. G. *Anal. Chem.* **1994**, *66*, 126−133.
(16) Dodonov, A. F.; Chernushevich, I. V.; Laiko, V. V. In *Time-of-flight mass spectrometry*; Cotter, R. J., Ed.; ACS Symposium Series 547; American Chemical Society: Washington, DC, 1994; p 108.
(17) Price, D. L.; Sköld, K. *Nucl. Instrum. Methods* **1970**, *82*, 208−222.
(18) Comsa, G.; David, R.; Schumacher, B. J. *Rev. Sci. Instrum.* **1981**, *52*, 789−796.
(19) Bewig, L.; Buck, U.; Gandhi, S. R.; Winter, M. *Rev. Sci. Instrum.* **1996**, *67*, 417−422.
(20) Nelson, E. D.; Fredman, M. L. *J. Opt. Soc. Am.* **1970**, *60*, 1664−1669.
(21) Harwit, M. D.; Sloane, N. J. *Hadamard Transform Optics*; Academic Press: London, 1979.
(22) Franzen, J. U.S. Patent 5,719,392, 1998.
(23) Riess, I. *Rev. Sci. Instrum.* **1987**, *58*, 784−787.
(24) Bailey, C. A.; Kilvington, J.; Robinson, N. W. *Vacuum* **1971**, *21*, 461−464.
(25) Knorr, F. J.; Ajami, M.; Chatfield, D. A. *Anal. Chem.* **1986**, *58*, 690−694.
(26) Knorr, F. J.; Eatherton, R. L.; Siems, W. F.; Hill, H. H., Jr. *Anal. Chem.* **1985**, *57*, 402−406.
(27) Meyerholtz, C. A.; Baer, R. L.; Coeq, C. A. L. U.S. Patent 5,396,065, 1995.
(28) Wiley, W. C.; MClaren, I. H. *Rev. Sci. Instrum.* **1955**, *26*, 1150−1157.

conventional space-focusing type of TOFMS is essentially impossible to operate in a full multiplexing mode over an extended mass range. The pair of grids cannot be pulsed sufficiently rapidly to accomplish this objective because of the time it takes for ions to drift into the region between the grids. Although some multiplexing can be achieved, the duty cycle of this instrument is much less than 50%. Moreover, this drift, of course, is mass dependent. For this reason, space focusing, which requires an extraction region defined by more than one grid, should be abandoned. In our design, we use a planar grid modulation scheme that allows much more rapid and mass-independent modulation.

The use of the Hadamard transform in chemical analysis has been reviewed by Treado and Morris.[29] Several books discussing transform techniques in chemistry are also available.[30−32] Hadamard transform methods have been used previously in mass spectrometry but in a rather different context, not involving multiplexing of the spectral elements. Williams et al.[33] performed FT-ICR MS/MS experiments on mixtures. They used the Hadamard scheme of weights to vary the composition of the mixture to aid the analysis.

DISCUSSION OF METHOD

Like any multiplexing scheme, HT-TOFMS relies on the modulation of an information carrier, in our case an ion beam, with some type of signal. In Hadamard spectroscopy, this signal is digital, which means that it has two states. Also, the signal is subjected to other constraints, which are fulfilled by using a pseudorandom sequence. The properties of these sequences are well understood.[21,34] Important for the experiment is that they are optimal or near-optimal, which means that the variance of the deconvoluted spectrum is a minimum. This feature guarantees that these pseudorandom sequences will produce the maximum or near-maximum possible improvement in the signal-to-noise ratio for this type of measurement.[18,21] The problem of how to reach the optimum has been solved in a generalized optimizing theory and depends on the structure, the total area of the spectrum, the background, and the duty cycle.[18] The optimum typically cannot be achieved because of practical limitations such as fixed duty cycle in the sequence generator or simply the spectral changes that accompany different samples.

Execution of the HT-TOFMS experiment is illustrated in Figure 1. The pseudorandomly encoded beam is made up of discrete ion packets containing all possible masses in the beam. The individual ion packets disperse by drifting through a field-free region. During their time of flight, lighter and therefore faster ions of later packets will overtake heavier and therefore slower ions from earlier released packets. At each instance in time, the signal generated by the detector represents the sum of ions having different masses. Figuratively speaking, the signal is the overlap of many time-of-flight distributions, each of which is shifted with respect to the start time of the modulation sequence. Mathematically, the signal is described as the convolution of the time-of-flight distribution and the pseudorandom sequence used for coding (chopping) the beam. To extract the time-of-flight distribution, a deconvolution step must be applied. So long as the modulation sequence is a pseudorandom sequence, this computation can be carried out essentially in real time with the help of a fast Hadamard transform algorithm.[20,21] Let us turn to the details of this procedure.

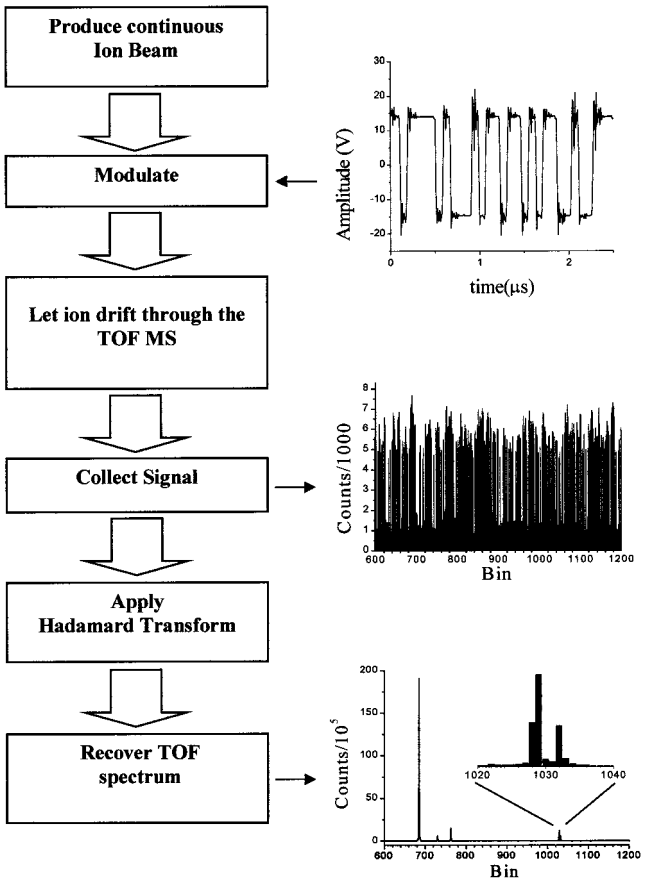

Figure 1. HT-TOFMS method flow chart. The left side shows the sequence of the steps in the procedure; the right side presents the actual performance of our apparatus when a solution of 25 mM cesium chloride in methanol is electrosprayed. The largest peak corresponds to Cs^+ followed by peaks for $Cs(H_2O)^+$, $Cs(CH_3OH)^+$, and Cs_2Cl^+ (which shows the 3:1 chlorine isotope ratio; see inset).

The convolution process that occurs in the in the experiment can be expressed succinctly in matrix notation as

$$\begin{bmatrix} \mathbf{Z} \end{bmatrix} = \begin{bmatrix} \mathbf{S} \end{bmatrix} \times \begin{bmatrix} \mathbf{T} \\ \mathbf{O} \\ \mathbf{F} \end{bmatrix} \qquad (1)$$

where **Z** is a vector representing the recorded signal, which is of dimension *n*, the length of the pseudorandom sequence. The quantity of interest is **TOF**, which is another vector of length *n* representing the time-of-flight distribution. The matrix **S** is an *n* × *n* matrix of ones (1's) and zeros (0's) known as the **S**-matrix. The columns of **S** are the pseudorandom sequence shifted by the column index with respect to the first column, making it a cyclic matrix. To recover the time-of-flight distribution **TOF** from the

(29) Treado, P. J.; Morris, M. D. *Anal. Chem.* **1989**, *61*, 723A−733A.
(30) Marshall, A. G.; Verdun, F. R. *Fourier Transforms in NMR, Optical, and Mass Spectrometry*; Elsevier: Amsterdam, 1990.
(31) Marshall, A. G., Ed. *Fourier, Hadamard, and Hilbert Transforms in Chemistry*; Plenum Press: New York, 1982.
(32) Griffiths, P. R., Ed. *Transform Techniques in Chemistry*; Modern Analytical Chemistry Series; Plenum Press: New York, 1978.
(33) Williams, E. R.; Loh, S. Y.; McLafferty, F. W.; Cody, R. B. *Anal. Chem.* **1990**, *62*, 698−703.
(34) Koleske, D. D.; Sibener, S. J. *Rev. Sci. Instrum.* **1998**, *63*, 3852−3855.

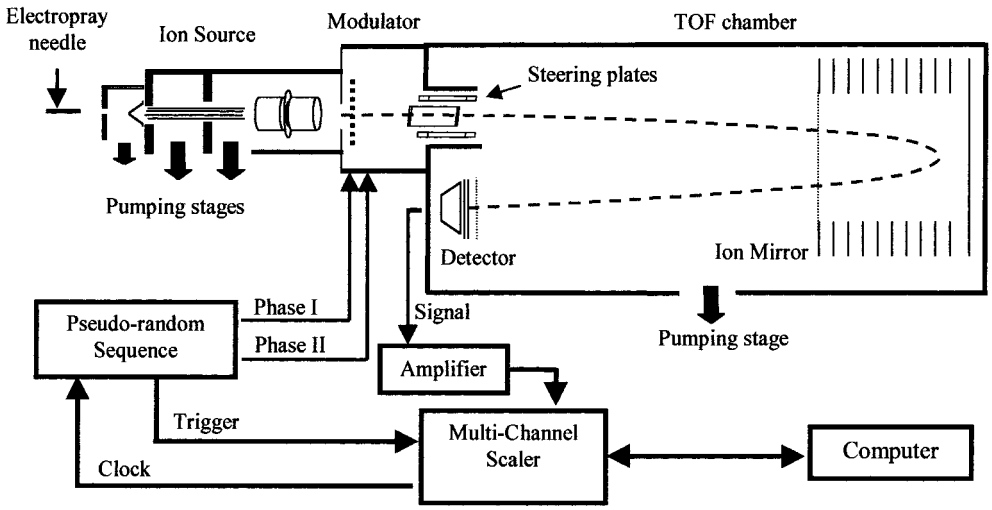

Figure 2. HT-TOFMS experimental setup.

signal **Z** we multiply both sides of eq 1 by $\mathbf{S^{-1}}$, the inverse of **S**, and obtain

$$\begin{bmatrix}\mathbf{T}\\ \mathbf{O}\\ \mathbf{F}\end{bmatrix} = \begin{bmatrix}\ \mathbf{S}\ \end{bmatrix}^{-1} \times \begin{bmatrix}\mathbf{Z}\end{bmatrix} \qquad (2)$$

The matrix $\mathbf{S^{-1}}$ is easily generated from **S** by replacing all 0's by $-1/k$ and all 1's by $1/k$, where k is the number of 1's in the pseudorandom sequence. Of course the normalization factor $1/k$ can be factored out of $\mathbf{S^{-1}}$. This factoring then leaves a matrix of only 1's and -1's, so that essentially the whole process involves only additions and subtractions, making it computationally fast. Furthermore, the number of operations can be reduced from n^2 to $2n + n \log_2 n$ by using a fast Hadamard transform algorithm described in the literature.[20,21] The length n of pseudorandom sequences is restricted to values of $2^m - 1$, where m is a positive integer. Consequently, the processing time necessary in going to the next larger sequence would increase by a factor of 4 in the direct matrix multiplication approach because the number of operations scales by n^2. The FHT requires little more than twice the number of operations for large n when going to the next larger **S**-matrix because of the $n \log_2 n$ scaling of the number of operations, making it vastly more efficient. Further, it can be computed that, for a typical **S**-matrix with $m = 13$, of dimension $(2^{13} - 1) \times (2^{13} - 1) = 8191 \times 8191$, the FHT will speed up computation by a factor of ~500 compared to direct matrix multiplication by $\mathbf{S^{-1}}$. The gains increase further with matrix size.

The multiplex gain G_M in the signal-to-noise ratio under shot-noise-limited conditions and negligible background over a conventional instrument transmitting only $1/n$ the number of ions is given by[17,35]

$$G_M = (x/2x_{av})^{1/2} \qquad (3)$$

where x is the intensity in the bin of interest and x_{av} is the average intensity across all bins. Equation 3 shows that gains through multiplexing under shot-noise-limited conditions are achievable for all bins in which x is at least 2 times the average spectral intensity x_{av}. This condition is generally fulfilled when the spectrum is sparse. Sparse spectra are usually encountered in mass spectrometry, so that multiplex gains should be expected. Moreover, the collinear arrangement and large acceptable beam size of a HT-TOFMS instrument should also produce an increase in throughput. The throughput gain G_{TP} in the signal-to-noise ratio is proportional to the square root of the increase in signal. The total gain G will then be the product of multiplex gain G_M and throughput gain G_{TP}. Under typical conditions, G is expected to be considerable, that is, a factor of 10−100, if not more, in the signal-to-noise ratio.

EXPERIMENTAL SECTION

Figure 2 illustrates the experimental setup of the HT-TOFMS system consisting of an ion source, a modulator, the TOF chamber, and the data acquisition system.

An ion beam is produced by a homemade electrospray ionization source (ESI) consisting of three differentially pumped stages. The vacuum coupling between atmospheric pressure and the first stage is done with a stainless steel capillary of 0.5-mm i.d. and of 85-mm length. The spray needle was a 30-gauge stainless steel capillary etched to a sharp tip at the end. The typical electrospray conditions were spray voltage of 2−3 kV, spray distance between the needle and the coupling capillary of 5−20 mm, nitrogen counterflow of 0.5 L/min, and a spray source temperature of 180 °C.

The ion source has an octopole ion guide that transports the ions through the second and third differentially pumped stages into the TOF chamber. Entering the time-of-flight instrument in collinear fashion, the beam is accelerated to energies ranging from 500 to 1250 eV and imaged by ion optics consisting of an ion lens and two sets of deflection plates onto a 9.5-mm-wide slit in front of the detector.

After the ion lens, a grid carries out the modulation of the beam. The modulator grid consists of interspersed wire sets positioned normal to the ion beam.[36] The wire sets are made from

(35) Larson, N. M.; Crosmun, R.; Talmi, Y. *Appl. Opt.* **1974**, *13*, 2662−2668.

(36) Vlasak, P. R.; Beussman, D. J.; Davenport, M. R.; Enke, C. G. *Rev. Sci. Instrum.* **1996**, *67*, 68−72.

20-μm-diameter gold-plated tungsten wire and spaced 158 μm apart.

The pseudorandom sequence generator is based on a 13-bit feedback shift register circuit[37] producing a sequence of length 8191. Two phases, 180° out of phase, are amplified in a home-built amplifier circuit and coupled capacitively onto the grid modulator wire sets, which floats at ±15 V with respect to the flight tube potential (−500 to − 1250 V). The ion beam passes undeflected when both wire sets are at the same potential, corresponding to the beam "on" state. When opposing potentials (±30 V between) are applied to the wire sets, the beam is split into two deflected beams, corresponding to the beam "off" state. In the "off" state, one-half of the ions are deflected slightly to one side, the other half slightly to the other side with respect to the undeflected beam, which causes the deflected ions to miss the detector slit. The effective drift path of the undeflected ions through the TOF chamber corresponds to 2.9 m. The reflectron used in the instrument is of the single-stage type. The ions, passing through the detector slit, are postaccelerated to an energy of 2000 eV before they are detected by a set of multichannel plates (MCPs).

The MCP output pulses are amplified and the signal is fed into a multichannel scaler for counting purposes. Synchronization of modulation and data acquisition is achieved by running the pseudorandom sequence generator from the clock (50 MHz) of the multichannel scaler. The multichannel scaler clock output is divided by 4 so that the sequence generator is clocked at 12.5 MHz, corresponding to the smallest "on" state duration of 80 ns. Data acquisition starts at a fixed point in the cycle of the modulation sequence and continues over the entire sequence for 655.28 μs. Decoding the shift register of the pseudorandom sequence generator generates the data acquisition start trigger. The data acquisition bin width in the multichannel scaler is set to 40 ns, half of the maximum size necessary to match the internal clock speed of the sequence generator because the scaler did not allow for an 80-ns bin width. The signal wave form acquired by the multichannel scaler is transferred to a computer, where pairs of successive bins are summed into bins of 80 ns width that match the modulation frequency. The inverse transform is than carried out by a program coded in C.

Calibration was achieved by measuring the mass spectrum of tetrabutylammonium perchlorate and using the known square root relationship between flight time and mass. Subsequently, the mass scale was refined by fitting to the multiply charged ion envelope of cytochrome *c*.

Solvents used for preparing the solutions were reagent grade. Cytochrome *c* (Sigma, St. Louis, MO), ubiquitin (Sigma), tetrabutylammonium perchlorate (Kodak, Rochester, NY), and cesium chloride (BRL, Gaithersburg, MD) were used as received without further purification. A solution of tetrabutylammonium perchlorate 146 μM in methanol was prepared and used as a standard. The concentration of the cesium chloride in methanol solution was 25 mM and contained 2% water. Cytochrome *c*, ubiquitin, and tetrabutylammonium perchlorate were dissolved in a methanol, water, and acetic acid mixture (65/30/5). Concentrations in the final solution were 37.2 μM for cytochrome *c*, 4.9 μM for ubiquitin, and 1.8 μM for tetrabutylammonium perchlorate.

(37) Horowitz, P.; Hill, W. *The Art of Electronics*, 2nd ed.; Cambridge University Press: Cambridge, U.K., 1989.

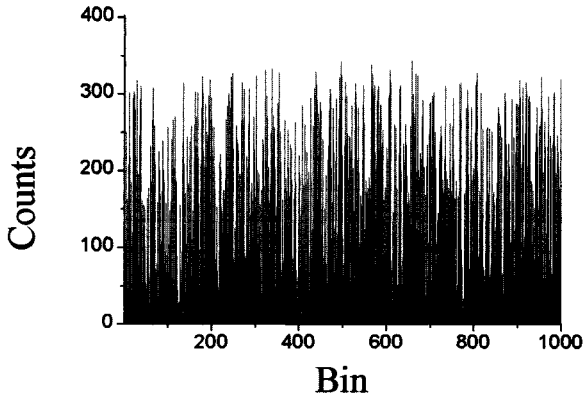

Figure 3. Signal wave form (first 1000 bins) of the spectrum shown in Figure 4.

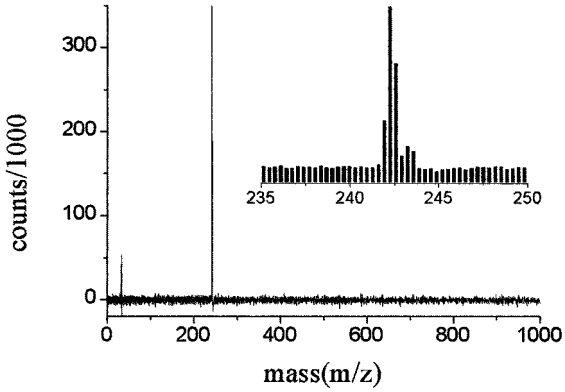

Figure 4. HT-TOF mass spectrum of electrosprayed 146 μM tetrabutylammonium perchlorate (acquisition time 32.75 s). The inset shows the expanded region from 235 to 255 amu.

RESULTS AND DISCUSSION

Figure 3 shows a recorded signal wave form. No identifiable structure is visible, which is of course expected when pseudorandom or pseudonoise modulation is employed. In the case of a single mass ion beam, the modulation sequence would be reproduced with some phase shift at the detector. Neglecting the background, there should be two types of bins: those with a fixed identical number of counts and those that are empty. This behavior is obviously not what is observed in Figure 3. Yet, from the depth of the wave form it is clear that there can be only a few or probably one dominating mass in the ion beam. Otherwise, the modulation depth would be expected to be much smaller. The dominance of a single mass in the recording of Figure 3 is apparent in Figure 4, which shows the inverse transform of Figure 3. The spectrum is the electrospray ionization mass spectrum of a 1.4×10^{-4} M solution of tetrabutylammonium perchlorate in methanol. The large peak at 242 amu is that of the tetrabutylammonium cation. A smaller peak at 33 amu also occurs and arises from protonated methanol. The inset in Figure 4 shows an expansion of the region around the tetrabutylammonium cation peak. There is a small feature visible at 243 amu that appears in all the spectra of this compound. This feature is attributed to an unknown impurity rather than an artifact because it is also present when a different modulation sequence is used. In several places small negative spikes are observed, the most pronounced appear-

ing next to the protonated methanol peak. These negative peaks are artifacts originating from systematic errors in the modulation. Modulation errors are of course correlated with the modulation sequences and produce therefore discrete noise spikes in the spectra, besides increasing the general background. A number of possible noise sources, their expression in the spectra, and the remedy thereof are discussed in the literature.[21,38] We are not performing any spectral correction in this study because the errors are quite small provided the instrument is properly tuned. Moreover, these spikes do not affect the interpretation of the mass spectrum.

The clean character of the spectrum shown in Figure 4 illustrates an important advantage of Hadamard transform over Fourier transform spectroscopy, which requires usually apodization of the interferogram before back transformation. Unapodized spectra tend to show ringing in the baseline and side lobes, both interfering with the interpretation of the spectrum. The origin of this problem lies in the basis functions used for FT analysis. Sine and cosine functions extend to plus and minus infinity and require for proper treatment a corresponding sampling interval, which is practically impossible to achieve. In Hadamard transform spectroscopy, this consideration is not an issue because the basis functions (Walsh functions)[21] are defined on the finite interval from $-^1/_2$ to $+^1/_2$, and therefore require only a limited sampling interval. Although, FT analysis is generally applicable to signals generated by a periodic modulation function, FT analysis is not optimal in cases where the modulation is not truly sinusoidal because significant amounts of signal can be located in overtones. This spreading out of the signal in multiple peaks reduces peak intensities and increases congestion in the spectra, both of which are very undesirable effects. This nonoptimal behavior was observed by Knorr[25] and accounts partly for his limited success. Last, FT analysis is made practical through the use of fast Fourier transform (FFT) algorithms. Yet, owing the absence of multiplication in the fast Hadamard transform (FHT), it will be generally ~10 times faster than an FFT of the same size. This speed advantage is especially important in applications were successive spectra need to be computed in real time without specialized processor boards. The time needed to compute the spectrum in Figure 4, for example, was 16 ms on our laboratory computer equipped with a Pentium processor running at 200 MHz.

The mass peak at 242 amu has a full width at half-maximum (fwhm) of two bins. The peak position is located at bin position 1486 in the spectrum, and the resolution $m/\Delta m$ equal to $t/2\Delta t$ in time of flight is calculated to be 372. Convolution of two boxcar functions, one representing an ideal square pulse generated by the modulator and the other an equal sampling bin width, results in a triangular-shaped peak with a fwhm of the bin width. From this idealized consideration, one could expect a fwhm resolution of 743 for the peak under consideration. The discrepancy with the experiment has experimental and sampling causes. Experimental limitations such as uncompensated kinetic energy spread in the beam and a limited rise time of the modulator potentials lead to a broadened ion pulse and therefore reduced resolution. The limiting sampling of the signal into bins of width equal to the pulse width will of course never allow for a triangular line shape and an accurate fwhm determination. A pulse sampled equally into two bins results in an fwhm of two bin widths or just half the theoretical resolution. Spectra recorded under different conditions clearly show the fwhm values vary between one and two bin widths. This sampling effect is clearly observable in the isotope pattern of the Cs_2Cl^+ peak shown as expansion in Figure 1. From these considerations we conclude that the instrument shows the expected mass resolution.

Peak definition can be increased by dividing the limiting sampling bin width into two, three, four, or more bins, which means the sampling rate must be increased by a multiple of the limiting sampling rate. Bin sequences of every second, third, fourth, or whatever multiple of the limiting sampling rate employed are then inverse transformed with the same transform used for a limiting sampled sequence. After inverse transformation, the sequences are interspersed again to give the final spectrum. The reader should be reminded that increasing the peak definition will not actually increase the time resolution, which is set by the smallest modulation pulse width.

The electrospray ionization mass spectrum of a mixture of two proteins, ubiquitin (4.9×10^{-6} M) and cytochrome *c* (3.7×10^{-5} M), is shown in Figure 5. The sprayed solution also contained a small amount of tetrabutylammonium perchlorate (1.8×10^{-6} M) as a standard. The characteristic envelope formed by the multiply charged ions of cytochrome *c* is the dominating feature. Charge states ranging from +19 to +10 of the 12 361 amu protein are visible. The observed envelope is typical for electrospraying from a solution of methanol/water/acetic acid with a ratio of 65/30/5.[14,15,39] The multiply charged ion peaks for ubiquitin (M_W ~8500 amu) are also visible. The peaks from charge state states +13 to +10 are recognizable. A negative noise spike appears at 616.2 amu and obscures possibly a feature around 618 that could be attributed to heme, a known impurity in cytochrome *c* according to one reviewer. We do not believe heme to be present because spectra recorded the previous day under different conditions show neither the negative spike nor a positive feature at this mass.

The theoretical uncertainty in the mass for a single peak is obviously limited by the bin width and decreases with $m^{-1/2}$. At 1000 amu, a single bin in the spectrum shown in Figure 5 covers 0.7 amu. For a multiply charged ion, this value must be multiplied by the charge state.

The acquisition time for this spectrum was 65.5 s at an average count rate of 158 700 counts/s. At a liquid flow rate of 1.7 μL/min, ~9 pmol of ubiquitin and 68 pmol of cytochrome *c* were consumed to produce the spectrum in Figure 5. These numbers can be compared with the work of Verentchikov,[15] who produced a spectrum of similar signal-to-noise ratio with only 50 fmol of cytochrome *c*. The causes for our low sensitivity are (a) lack of optimization of the electrospray source, (b) the rather low resolution of the instrument at this time, and (c) an insufficient deflection of the ion beam in the "off" state, which increases the background noise and reduces the effective signal level thereby losing a large part of the expected multiplex gain. Scanning of the beam image over the detector slit indicates that an increase of the deflection voltage to ±50 V should suffice to remedy (c). The rise time of the voltage pulses applied to the modulator are

(38) Zeppenfeld, P.; Krzyzowski, M.; Romainczyk, C.; David, R. *Rev. Sci. Instrum.* **1993**, *64*, 1520−1523.

(39) Bodarenko, P. V.; Macfarlane, R. D. *Int. J. Mass Spectrom. Ion Processes* **1997**, *160*, 241−258.

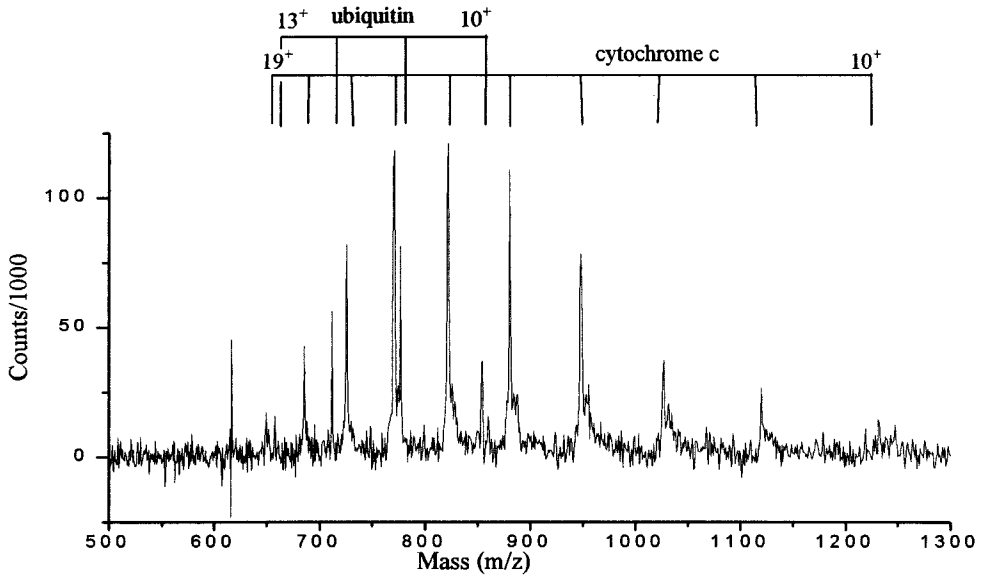

Figure 5. HT-TOF mass spectrum of an electrosprayed mixture of 37.2 μM cytochrome *c* and 4.9 μM ubiquitin (acquisition time 65.5 s).

~12 ns. This degrades the shape of the ion pulses and introduces additional noise into the spectrum. But, even with an infinite rise time, the pulse edges would still be degraded because the deflection region has a finite size estimated by simulations to be ~60% of the wire spacing. The edges off the ion pulses cannot be sharper than the time it takes for the ions to travel through this interaction region. A 1000 amu ion accelerated to a kinetic energy of 1000 eV will pass through the interaction region of our present grid in ~7 ns. This calculation shows that some improvement can be achieved by sharpening the edges of the voltage pulses but that the final limitations are the physical dimensions of the modulator under our typical accelerating voltages, desired resolutions, and instrument size. Further, the degradation of the edges is mass dependent, higher ion mass pulses being affected more strongly owing to their slower speeds. As a consequence, the noise in the spectrum will be generally higher when considerable amounts of high-mass species are present in the ion beam. We believe at present that (a) and (c) are the chief contributions to a lack of sensitivity. If so, large gains in sensitivity should be readily obtained by improving the ion source and the modulator with its associated circuitry. Experiments are underway in hopes of demonstrating these gains.

CONCLUSIONS AND PROSPECTS

The feasibility of Hadamard transform time-of-flight mass spectrometry has been demonstrated, and it has been applied to the mass analysis of a mixture of biomolecules. Key features of HT-TOFMS are high duty cycle (50 or 100%) and high ion throughput owing to acceptable ion beam sizes of several millimeters. In addition, a major instrumental advantage over orthogonal extracting TOFMS is achieved through the collinear arrangement of ion source and mass spectrometer, which allows ease of coupling to various separation methods. Several shortcomings of the present system have also been identified. Work is in progress to improve the time resolution of the instrument and the separation of the "on" and "off" states.

HT-TOFMS allows simple and efficient coupling of continuous ion beams to TOFMS, which has the potential of making this scheme a low-cost, general-purpose detector for coupling to various electrophoretic, electrokinetic, and chromatographic separations. Moreover, the gain in the signal-to-noise ratio, which arises from both the multiplexing gain and the throughput gain, may give Hadamard transform time-of-flight mass spectrometry unique advantages in many applications for which sensitivity, fast data acquisition, and versatility are required.

ACKNOWLEDGMENT

This work was supported by Beckman Instruments, Inc.

Received for review April 13, 1998. Accepted June 26, 1998.

AC9804036